Stability and Aromaticity of B_iN_i Rings and Fullerenes

Jon M. Matxain,*,† Jesus M. Ugalde,† M. D. Towler,‡ and R. J. Needs‡

Kimika Fakultatea, Euskal Herriko Unibertsitatea, P.K. 1072, 20018 Donostia, Euskadi, Spain, and Cavendish Laboratory, Madingley Road, Cambridge CB3 0HE, United Kingdom

Received: August 5, 2003

B_iN_i clusters have been studied using the hybrid B3LYP density functional and diffusion quantum Monte Carlo (DMC) methods. Different cluster families have been characterized for each cluster size using B3LYP, and the energy differences have been compared with those obtained within DMC. The DMC results predict that the global minimum energy structures are rings for $i = 2-9$, a three-ring structure for $i = 10$ and spheroids for $i \geq 11$. The aromaticity of the ring structures has been studied using the nuclear independent chemical shifts (NICS) criterion. According to this criterion, rings with an odd number of BN units are aromatic. Aromatic structures are thought to be the most stable, and the DMC results for the most stable structures are consistent with this hypothesis, but in some cases, the B3LYP results are not.

1. Introduction

Over 40 years ago, Richard Feynman described how in nanotechnology "There's plenty of room at the bottom!".[1] Indeed, the recent spectacular growth of nanotechnology has followed the predictions of some of the pioneers in the field, such as Arthur von Hippel[2] and K. Eric Drexler.[3,4] There have been many important developments in nanotechnology,[5−8] and new and revolutionary techniques have been developed, such as the scanning tunneling microscope (STM), the atomic force microscope (AFM), and others. It might be possible to create new materials that are useful in a broader sense than their bulk counterparts.[9−13] The recent spectacular success of nanotechnology makes cluster science more interesting, because in addition to rationalizing some surface-related and other properties of bulk materials, studies of clusters of increasingly larger sizes can eventually bridge the gap with nanosize materials in a comprehensible manner. Consequently, the literature in the field is growing rapidly, and several reviews of cluster science have appeared.[14−16] One of the best known "new" clusters or nanostructures is the family of so-called fullerenes discovered in 1985,[17] which are hollow carbon spheroidal structures.

Interest in valence isoelectronic clusters such as III−V clusters is also growing rapidly. Studies of small III−V clusters have appeared in the literature,[18−21] along with studies of large clusters or bulk.[22−24] III−V fullerenes and nanotubes have also been studied.[25−28] Theoretical studies have been performed for fullerene-like $B_{12}N_{12}$ clusters,[29,30] in which it has been found that a structure built from squares and hexagons is more stable than those built from pentagons and hexagons. This is because in the second case less stable B−B and N−N bonds are formed. The most stable $B_{12}N_{12}$ structure is built from six squares and eight hexagons. The $B_{36}N_{36}$ fullerene has also been studied theoretically,[31] and a structure built from six squares and 32 hexagons has been found. Similar structural trends have been observed for II−VI clusters,[32] in which fullerene-like structures are built from six squares with the number of hexagons increasing by one when adding a new unit.

In this work, we focus on B_iN_i clusters, $i = 2-15$. Our aim is to find the global minimum energy structure for each cluster size, for which an exhaustive search of the potential energy surface has been performed. To characterize the cluster geometries, we use the hybrid B3LYP exchange-correlation functional within density functional theory. However, energy differences obtained within density functional theory may not be as accurate as one would like, and therefore, when the energy differences are small, we have performed diffusion quantum Monte Carlo (DMC) calculations. This level of accuracy has been found to be crucial for accurate studies of the crossover from carbon rings to fullerenes.[33]

The DMC method[34,35] is the most accurate approach known for calculating the quantum-mechanical ground-state energy of a large number of interacting particles. The great promise of DMC for interacting electron systems lies in the fact that correlations are included explicitly and that the computational cost increases as the third power of the number of electrons, which is very favorable when compared with other correlated wave function techniques. Highly accurate DMC calculations have already been demonstrated for both molecules[33,36−39] and condensed matter systems.[34,40−42]

2. Methods

All geometries were fully optimized using the hybrid[43] Becke 3 Lee−Yang−Perdew (B3LYP) gradient-corrected approximation within density functional theory.[44−46] Harmonic vibrational frequencies were determined by analytical differentiation of the energy gradients, and we checked that all of the optimized structures have only positive force constants.

We used soft pseudopotentials[47] to model the core electrons, which are important for efficient quantum Monte Carlo calculations. These pseudopotentials were combined with an efficient uncontracted Gaussian basis set for the valence electrons, which contains five s-type, five p-type and one d-type functions for both B and N. The values of the exponents are given in Table 1.

The reliability of the energy differences obtained with this method has been tested using two all-electron basis sets, namely, 6-311G(d)[48,49] and a TZ2P. Single-point calculations have been

† Euskal Herriko Unibertsitatea.
‡ Cavendish Laboratory.

10.1021/jp036296n CCC: $25.00
Published on Web 10/24/2003

TABLE 1: Basis Set Exponents for the B and N Atoms in au

	B α	N α
s	52.5393	68.6151
s	8.5622	12.679
s	2.003	3.0226
s	0.5749	1.026
s	0.1916	0.418
p	6.3999	6.7365
p	1.5767	1.4646
p	0.3856	0.4257
p	0.1018	0.1431
p	0.0303	0.0524
d	0.8	0.8

TABLE 2: Energy Differences (eV) for the Lowest-Lying Structures of the B_iN_i, $i = 2$ and 3, Clusters Using Three Different Basis Sets

	this work	6-311G(d)	TZ2P
ΔE ($E_{B_2N_2}{}^{GM} - E_{B_2N_2}{}^{LM1}$)	0.283	0.430	0.517
ΔE ($E_{B_3N_3}{}^{GM} - E_{B_3N_3}{}^{LM1}$)	4.185	4.411	4.370

carried out with these basis sets because the geometry of the clusters was not significantly altered by optimizing the structures with each basis set. The results obtained are given in Table 2.

Each of the basis sets predicts the same global minimum energy structure, and the estimated energy differences are similar, which supports the reliability of our pseudopotential−basis set combination.

The nuclear independent chemical shifts (NICS) values were calculated using the gauge-including atomic orbitals (GIAO) method at the B3LYP level of theory. In this method, the nuclear magnetic resonance (NMR) parameters are calculated for a ghost atom, usually placed at the center of the ring, and the NICS value is the negative of the isotropic magnetic shielding constant at the ghost atom. The aromaticity of a ring structure can be studied by computing the NICS value in the center of the structure, either in the plane of the ring or 1 Å out of the plane, which are generally denoted as NICS(0) and NICS(1), respectively. If the corresponding NICS values are negative, the structure is aromatic.[50,51]

In the DMC method,[34,35] the imaginary time Schrödinger equation is used to evolve an ensemble of electronic configurations toward the ground state. Exact imaginary-time evolution would lead to the exact fermion ground-state wave function, provided it has a nonzero overlap with the initial fermion state. However, the stochastic evolution is never exact, and the solution converges to the bosonic ground state. In DMC calculations, the fermionic symmetry is maintained by the fixed-node approximation,[52] in which the nodal surface of the wave function is constrained to equal that of a guiding wave function. The fixed-node DMC energy provides a variational upper bound on the ground-state energy with an error that is second-order in the error in the nodal surface.[53,54]

In this work, Slater−Jastrow-type guiding wave functions consisting of the product of a Slater determinant of single-particle orbitals obtained using the Gaussian 98 code[55] and a Jastrow correlation factor[56] have been used. The optimized uncontracted basis set of Table 1 has been used to generate single-particle Hartree−Fock orbitals, which form the Slater determinant of the guiding wave function. We emphasize that the DMC energies are not limited by the basis set or the detailed form of the orbitals, the DMC energy is fixed only by the nodal surface of the guiding wave function. The Jastrow factors, up to 25 parameters, were optimized using efficient variance minimization techniques.[57,58] All of the DMC calculations were performed using the CASINO code.[59]

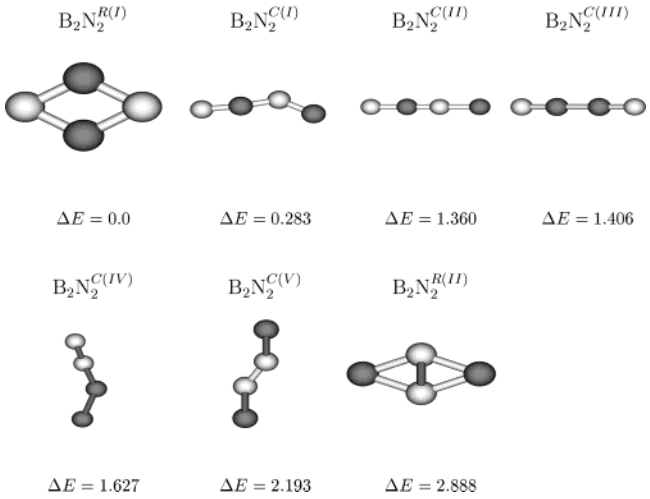

Figure 1. Cluster structures characterized for B_2N_2. Shaded atoms are B.

Although the computational effort of a DMC calculation scales as the cube of the number of electrons, the scaling with the atomic number, Z, of the atoms is approximately $Z^{5.5-6.5}$.[60,61] It is therefore very advantageous to use pseudopotentials in DMC calculations, which reduces the effective value of Z. Hartree−Fock pseudopotentials have been shown to give better results than density functional theory ones when used within DMC calculations.[62] Unfortunately, the Hartree−Fock pseudopotentials available within the quantum chemistry literature usually diverge at the origin, normally like $1/r^2$ or $1/r$. These divergences lead to large "time-step" errors and even instabilities in DMC calculations.[63] In this study, we have used soft pseudopotentials,[47] which are smooth at the origin and do not suffer from this problem. The nonlocal energy was evaluated stochastically within the locality approximation.[64−66]

3. Results

This section has been organized as follows. In subsection 3.1, the structures characterized at the B3LYP level of theory are presented. Subsection 3.2 deals with the aromaticity of some planar structures, and finally the DMC results are reported in subsection 3.3.

3.1. Structures of the B_iN_i clusters, $i = 2-15$. The structures can be divided into different families, namely, rings, chains, two-rings, three-rings, five-rings, graphitic-like and three-dimensional spheroids. The structures are labeled according to the following system: $B_iN_i{}^a$, where i denotes the number of BN units and the superscript a denotes the family of the structure. The families are R (rings), C (chains), S (spheroids), 2R (two-rings), 3R (three-rings), 5R (five-rings), G (graphitic), D (distorted spheroids), and O (others).

B_iN_i, $i = 2-5$. The optimized structures for $i = 2-5$ are shown in Figures 1 ($i = 2$) and 2 ($i = 3-5$), along with the energy differences in electronvolts of each structure from the most stable one. For B_2N_2, the three most stable structures contain only B−N bonds, while higher lying structures contain B−B or N−N bonds. This is in agreement with previous work on BN clusters.[28,29] Therefore, for larger clusters, only completely B−N bonded structures are shown. The global minimum energy structure is found to be a ring, while a bent chain lies close in energy. It is interesting to note that this bent chain is preferred to a linear chain. The bent chain is only 0.283 eV above the global minimum, while the linear one is 1.360 eV above. As the cluster size increases, the energy difference

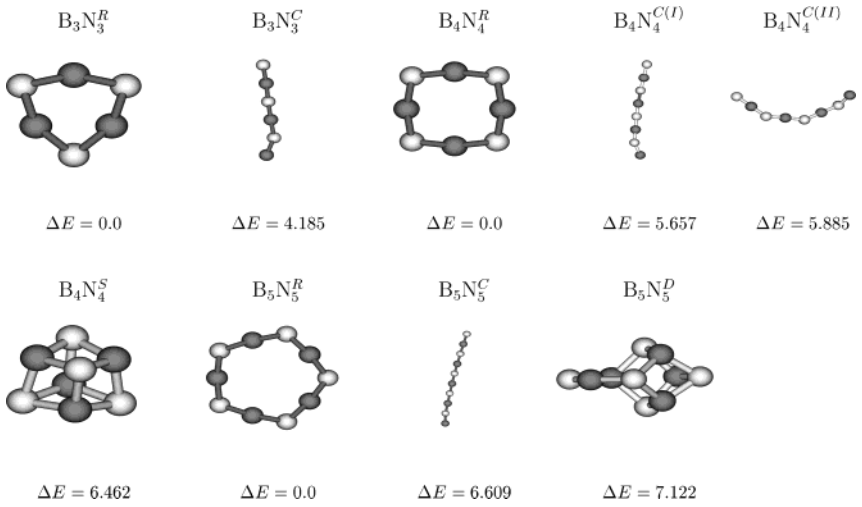

Figure 2. Cluster structures characterized for B_iN_i, $i = 3-5$.

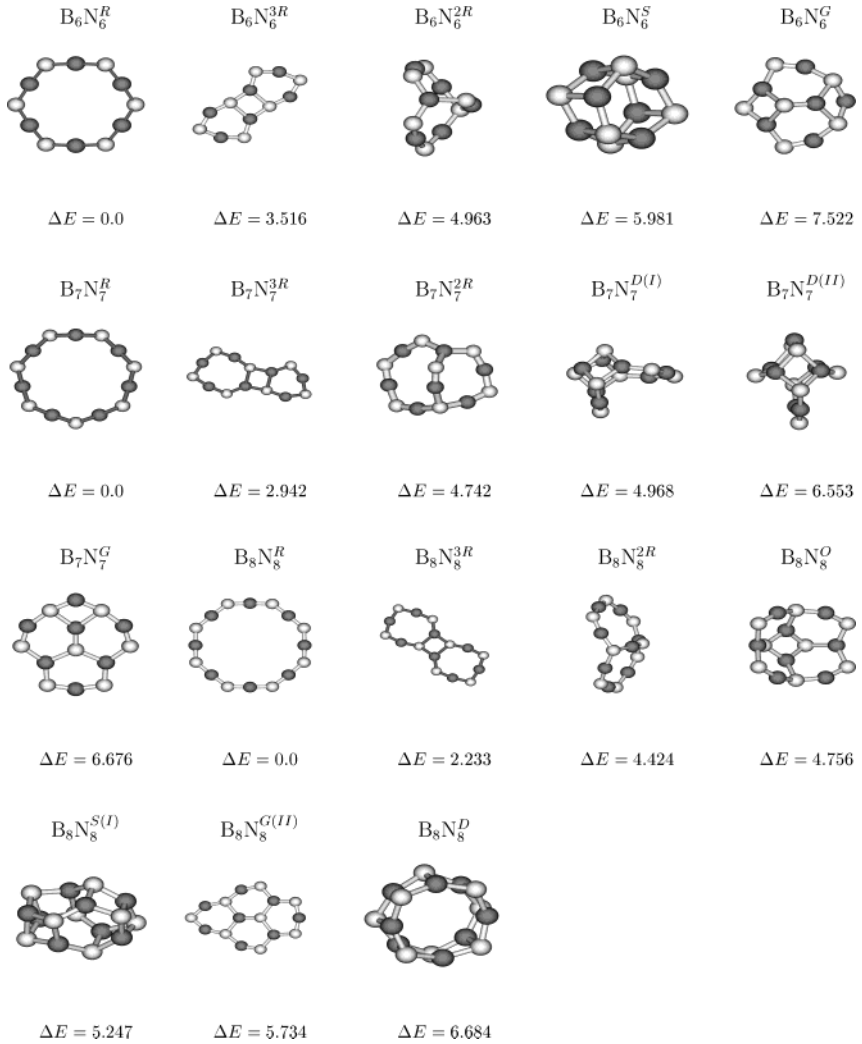

Figure 3. Cluster structures characterized for B_iN_i, $i = 6-8$.

between the ring and chain structure increases, being 4.185, 5.657, and 6.609 eV for $i = 3$, 4, and 5, respectively. In ring structures, a strong tendency toward N−B−N angles of 180° is observed as the cluster size increases. Three-dimensional structures have also been characterized for $i = 4$ and 5. $B_4N_4^S$ is interesting, although it is very high in energy (6.462 eV above the minimum) because it is composed of six squares and is a deformed cube. This is the smallest spheroid following the so-called squares−hexagons route. $B_5N_5^D$ lies even higher in energy than $B_4N_4^S$.

B_iN_i, $i = 6-11$. The optimized structures for $i = 6-11$ are shown in Figures 3 ($i = 6-8$) and 4 ($i = 9-11$), along with the energy differences from the most stable structures in electronvolts. For all cluster sizes, the global minima are ring

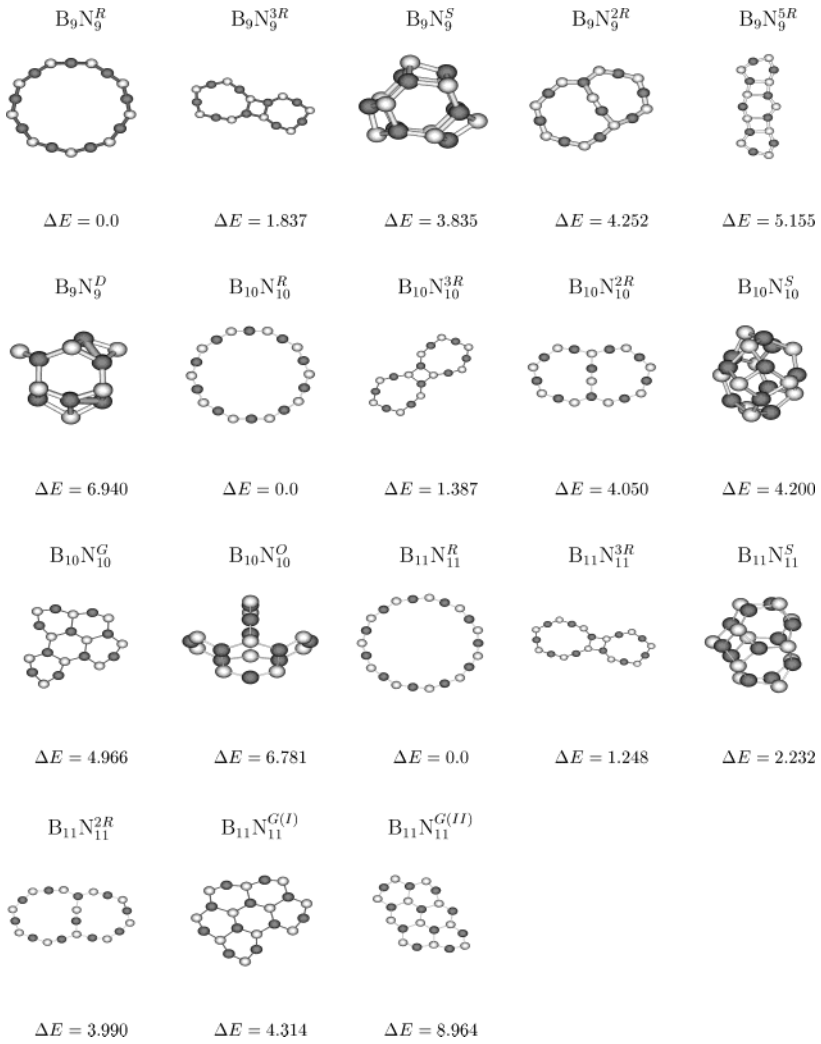

Figure 4. Cluster structures characterized for B_iN_i, $i = 9-11$.

structures with N−B−N angles close to 180°. In smaller clusters, we have shown above that the chain structures lie higher in energy as *i* increases, and therefore, we have not characterized them for these cluster sizes. On the other hand, new families of structures are observed at these cluster sizes. The lowest-lying local minimum energy structures belong to the three-ring family, in which two rings are linked together by a small square. The energy differences decrease as *i* increases, being 3.516 eV for $i = 6$ and 1.248 eV for $i = 11$. The two-ring family is the second lowest-lying local minimum and spheroids the third one, except for $i = 11$, for which the spheroid is closer to the global minimum. In the case of two-ring structures, the energy difference decreases from 4.963 eV ($i = 6$) to 3.990 eV ($i = 11$) and in the case of spheroids from 5.981 eV ($i = 6$) to 2.232 eV ($i = 11$). The graphitic-like structures and distorted spheroids lie about 6 eV higher in energy and are not described in detail.

B_iN_i, $i = 12-15$. The optimized structures for $i = 12-15$ are shown in Figure 5, along with the energy differences of these structures from the most stable one in electronvolts. We observe a transition in the global minimum structures, which are spheroids for $i = 12$, 14, and 15. However, for $i = 13$, the ring structure is predicted to be the global minimum. Except for $i = 15$, the energy differences between spheroids and rings are small, and a more accurate picture is desirable.

Spheroids are built from squares and hexagons. The number of squares remains constant and equal to six, while the number of hexagons increases as the cluster size increases. A similar trend is observed in carbon fullerenes, where the number of pentagons remains constant at twelve, while the number of hexagons increases with cluster size. These trends can be seen in Table 3.

In ref 31, a $B_{36}N_{36}$ fullerene was characterized, built from six squares and 32 hexagons, which follows our trend rather nicely. This trend was also observed in II−VI clusters[32] and is common for all structures built from squares and hexagons.

In Figure 6, all energies of each structural family, relative to the rings, are depicted as a function of the cluster size. We observe that rings are the global minimum structures for $i = 2-11$ and 13 and spheroids are the global minimum structures for $i = 12$, 14, and 15. In the small cluster size region, $i = 2-5$, rings clearly dominate, except for $i = 2$, for which the chain structure lies close in energy. Then, as the cluster size increases, the energy differences of all of the families decreases, specially that of spheroids, which become the most stable structures for larger cluster sizes. The three-ring structures also lie close in energy for large cluster sizes. DMC calculations will provide a more accurate picture of the relative energies for regions where different structures lie close in energy, see subsection 3.3. The structures chosen for the DMC calculations are the ring and chain for $i = 2$, and rings, three-rings, and spheroids for $i = 8-13$.

3.2. Aromaticity in B_iN_i Rings. The aromaticity of these rings has been studied using the NICS method, which is a magnetic criterion that mirrors the ring current. The NICS values

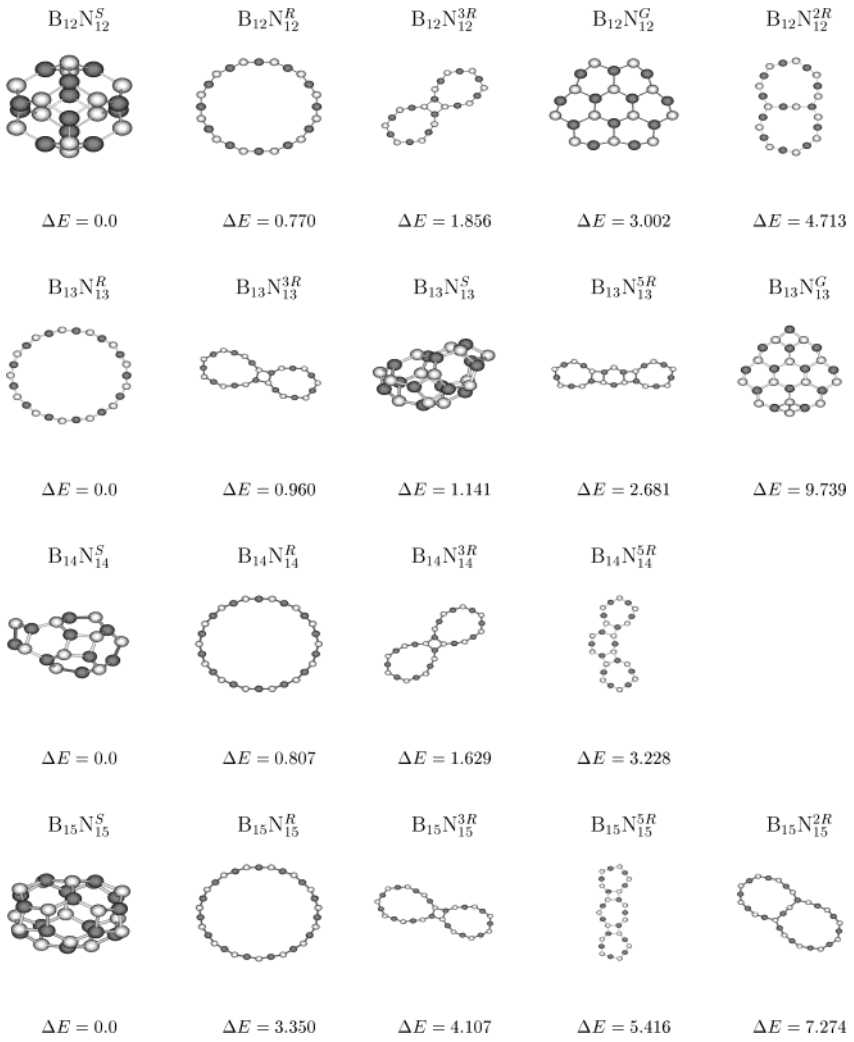

Figure 5. Cluster structures characterized for B_iN_i, $i = 12-15$.

TABLE 3: Structural Trends in BN Spheroids and Fullerenes

	$B_4N_4^S$	$B_6N_6^S$	$B_8N_8^S$	$B_9N_9^S$	$B_{10}N_{10}^S$	$B_{11}N_{11}^S$	$B_{12}N_{12}^S$	$B_{13}N_{13}^S$	$B_{14}N_{14}^S$	$B_{15}N_{15}^S$
squares	6	6	6	6	6	6	6	6	6	6
hexagons	0	2	4	5	6	7	8	9	10	11

	C_{20}	C_{28}	C_{34}	C_{42}	C_{48}	C_{54}	C_{60}	C_{72}	C_{84}	C_{94}
pentagons	12	12	12	12	12	12	12	12	12	12
hexagons	0	4	7	11	14	17	20	26	32	37

are easily calculated as the negative of the magnetic shielding. Negative values arise when diatropic ring currents dominate, that is, aromaticity, while positive values arise when paratropic currents dominate, that is, antiaromaticity. The NICS(0) value, calculated at the center of the ring, is influenced by the σ-bonds, and therefore, calculation of the NICS(1), 1 Å out of the plane, yields a more reliable result because these values are mainly influenced only by the π system.[51] The results obtained are given in Table 4.

These results indicate that rings with odd values of i are aromatic and those with even values of i are antiaromatic, except for $i = 2$. As the size of the ring increases the aromaticity decreases, $B_7N_7^R$ being the largest aromatic ring. $B_iN_i^{3R}$ structures are built from two B_iN_i rings linked together by a B_2N_2 ring. It has been shown above that the $B_iN_i^R$ structures with $i = 2$, 3, 5, and 7 are aromatic, so in principle, they can maintain their aromaticity within the $B_iN_i^{3R}$ structures. The NICS(1) values have been calculated 1 Å above the center of each of the rings, and therefore, for the same structure, three values are provided in Table 5, corresponding to each of the indicated rings.

The results in Table 5 show that only B_iN_i, $i = 3$ and 5, rings within $B_iN_i^{3R}$ structures are aromatic. Comparing these results with those of Table 4, we see that the aromaticity of these rings decreases from isolated rings to rings within $B_iN_i^{3R}$ structures. In this way, isolated $B_2N_2^R$ and $B_7N_7^R$ are aromatic, but they are antiaromatic when fused with other rings within $B_iN_i^{3R}$ structures. Similarly, notice that for all even-i rings the antiaromaticity increases compared with their corresponding values for isolated rings.

3.3. DMC Calculations for B_iN_i, $i = 2$ and 8−13. As mentioned above, the structures chosen for the DMC calculations are the ring and chain for $i = 2$ and rings, three-rings, and spheroids for $i = 8-13$. Smaller structures are not considered because the energy differences between the rings and other structures are very large. Although the extra accuracy of DMC could alter the energy differences, it is not expected to change the global minimum structures. The relative energies

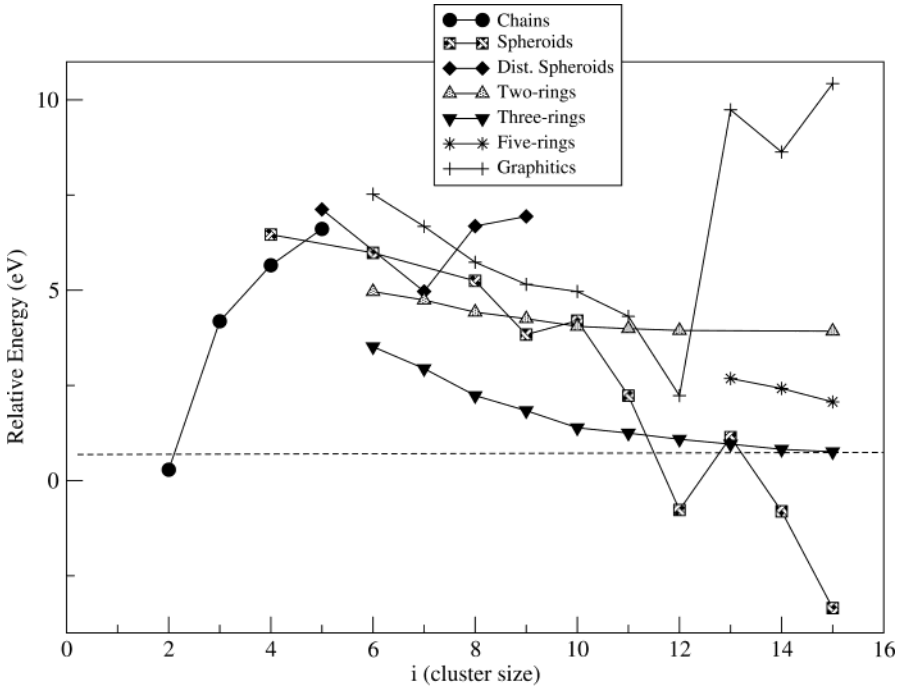

Figure 6. Energy differences between the ring and the remaining structures in kJ/mol at the B3LYP level of theory.

TABLE 4: NICS(0), Calculated in the Center of the Ring, and NICS(1), Calculated 1 Å out of the Plane, Values for $B_iN_i^R$ Structures

	NICS(0)	NICS(1)
$B_2N_2^R$	−54.4050	−10.8124
$B_3N_3^R$	−11.5038	−2.7952
$B_4N_4^R$	0.7791	1.8903
$B_5N_5^R$	−2.8316	−2.0540
$B_6N_6^R$	0.3597	0.6063
$B_7N_7^R$	−0.8899	−0.5512
$B_8N_8^R$	0.6361	0.6629
$B_9N_9^R$	0.2419	0.2963

TABLE 5: NICS(1) Values, Calculated 1 Å out of the Plane, for $B_iN_i^{3R}$ Structures

	B_2N_2	B_3N_3	B_4N_4	B_5N_5	B_6N_6	B_7N_7
$B_6N_6^{3R}$	4.0099	−0.8808				
$B_7N_7^{3R}$	3.2465	−1.4252	0.4509			
$B_8N_8^{3R}$	3.3365		0.8901			
$B_9N_9^{3R}$	4.3317		1.1618	−1.0496		
$B_{10}N_{10}^{3R}$	5.7349			−0.9540		
$B_{11}N_{11}^{3R}$	5.3311			−0.8937	5.3311	
$B_{12}N_{12}^{3R}$	5.1594				1.1558	
$B_{13}N_{13}^{3R}$	6.1075				1.1420	0.8856
$B_{14}N_{14}^{3R}$	6.9706					0.9014

TABLE 6: Calculated Energy Differences, ΔE, in EV, at the B3LYP and DMC Levels of Theory

	B3LYP	DMC
ΔE ($E_{B_2N_2^R} - E_{B_2N_2^C}$)	+0.283	+1.392 ± 0.055
ΔE ($E_{B_8N_8^R} - E_{B_8N_8^{3R}}$)	+2.233	+1.541 ± 0.160
ΔE ($E_{B_9N_9^R} - E_{B_9N_9^{3R}}$)	+1.837	+2.227 ± 0.123
ΔE ($E_{B_{10}N_{10}^R} - E_{B_{10}N_{10}^{3R}}$)	+1.387	−1.685 ± 0.127
ΔE ($E_{B_{10}N_{10}^R} - E_{B_{10}N_{10}^S}$)	+4.200	+2.081 ± 0.172
ΔE ($E_{B_{11}N_{11}^R} - E_{B_{11}N_{11}^S}$)	+2.232	−1.490 ± 0.151
ΔE ($E_{B_{11}N_{11}^R} - E_{B_{11}N_{11}^{3R}}$)	+1.248	+2.557 ± 0.223
ΔE ($E_{B_{12}N_{12}^R} - E_{B_{12}N_{12}^S}$)	−0.770	−7.750 ± 0.169
ΔE ($E_{B_{13}N_{13}^R} - E_{B_{13}N_{13}^S}$)	+1.141	−4.412 ± 0.178

calculated in DMC and B3LYP are compared in Table 6. For the $i = 2$ case, DMC confirms the B3LYP result, in which the ring is more stable than the chain. For larger clusters, $i = 8-13$, the results have to be discussed in a deeper way. First of all, recall that $B_iN_i^R$ structures are predicted not to be aromatic for $i \geq 8$, while $B_iN_i^{3R}$, $i = 9-11$, have aromatic components, which are the B_5N_5 rings. For $i = 8$ and 9, DMC and B3LYP results are in agreement, and both predict $B_iN_i^R$ clusters to be the global minima. The case of $i = 10$ is different. DMC predicts $B_{10}N_{10}^{3R}$ to be the global minimum, which has two aromatic B_5N_5 rings, while B3LYP predicts the antiaromatic $B_{10}N_{10}^R$ to be most stable. The results of the DMC calculations are therefore in agreement with the aromaticity picture. For larger cases, $i \geq 11$, DMC calculations predict spheroids to be the global minima. Therefore, according to our DMC results, ring structures are the global minima for $i = 2-9$, the three-ring structure is the global minimum for $i = 10$, and spheroids are the global minima for $i \geq 11$.

4. Conclusions

The hybrid B3LYP functional has been used to characterize the geometry of a number of different structural families for a wide range of cluster sizes. Although density functional theory usually predicts reasonable bond lengths and bond angles, the calculated energy differences are not particularly accurate because of the approximate exchange-correlation functionals used. At this point, the importance of diffusion quantum Monte Carlo (DMC) calculations is clear because it is crucial to determine the correct global minima for B_iN_i clusters. B3LYP predicts ringlike structures to be the global minima for $i = 2-11$ and 13 and spheroids for $i = 12$, 14, and 15. In the region of the crossover from rings to spheroids, DMC calculations show a different sequence, the global minima structures being ringlike for $i = 2-9$, three-ring structures for $i = 10$, and spheroids for $i = 11-15$. This difference comes from the fact that DMC describes correctly the correlation energy for all systems, while B3LYP does not. In this case, B3LYP underestimates the energy of the spheroids.

The aromaticity of the $B_iN_i^R$ and the $B_iN_i^{3R}$ structures has been studied using the nuclear independent chemical shifts (NICS) criterion. According to this criterion, $B_iN_i^R$, $i = 2$, 3, 5, and 7, are aromatic, while within $B_iN_i^{3R}$ structures, only $i = 3$ and 5 rings are aromatic. In this case, the $B_{10}N_{10}^{3R}$ structure is

built from two aromatic rings linked together by a square, and because of these aromatic rings, the stability of this structure is large. These results for aromaticity are consistent with the DMC results for the most stable structures because aromatic structures are thought to be the most stable.

Acknowledgment. J.M.M. and J.M.U. thank the University of the Basque Country and Ministerio de Educacion y Ciencia for financial support. M.D.T. thanks the Royal Society for a Research Fellowship, and R.J.N. thanks the Engineering and Physical Sciences Research Council (U.K.) for funding.

References and Notes

(1) Feynman, R. P. *Eng. Sci.* **1960**, *23*, 22. Reprinted in *Miniaturization*; Gilbert, H. D., Ed.; Reinhold: New York, 1961; p282.
(2) von Hippel, A. R. *Science* **1962**, *138*, 91.
(3) Drexler, K. E. *Proc. Natl. Acad. Sci. U.S.A.* **1981**, *78*, 5275.
(4) Drexler, K. E. *Engines of Creation*; Doubleday: New York, 1986.
(5) Zach, M. P.; Ng, K. H.; Penner, R. M. *Science* **2000**, *290*, 2120.
(6) Joachim, C.; Gimzewski, J. K.; Aviram, A. *Nature* **2000**, *408*, 541.
(7) Chadwick, A. V. *Nature* **2000**, *408*, 925.
(8) Sata, N.; Eberman, K.; Eberl K.; Maier, J. *Nature* **2000**, *408*, 946.
(9) Craighead, H. G. *Science* **2000**, *290*, 1532.
(10) Quake S. R.; Schrerer, A. *Science* **2000**, *290*, 1536.
(11) Jager, E. W. H.; Smela E.; Inganäs, O. *Science* **2000**, *290*, 1540.
(12) Paiella, R.; Capasso, F.; Gmachi, C.; Sivco, D. L.; Baillargeon, J. N.; Hutchinson, A. L.; Cho, A. Y.; Liu, H. C. *Science* **2000**, *290*, 1739.
(13) Suenaga, K.; Tencé, M.; Mory, C.; Colliex, C.; Kato, H.; Okazaki, T.; Shinohara, H.; Hirahara, K.; Bandow, S.; Lijima, S. *Science* **2000**, *290*, 2280.
(14) Jortner, J. *Z. Phys. D* **1992**, *24*, 247.
(15) Castleman, A. W., Jr.; Bowen, K. H., Jr. *J. Phys. Chem.* **1996**, *100*, 12911.
(16) Hartke, B. *Angew. Chem., Int. Ed.* **2002**, *41*, 1468 and references therein.
(17) Kroto, H. W.; Head, J. R.; O'Brien, S. C.; Curl, R. F.; Smalley, R. E. *Nature* **1985**, *318*, 162.
(18) Kandalam, A. K.; Blanco, M. A.; Pandey, R. *J. Phys. Chem. B* **2002**, *106*, 1945.
(19) Costales, A.; Kandalam, A. K.; Franco, R.; Pandey, R. *J. Phys. Chem. B* **2002**, *106*, 1940.
(20) BelBruno, J. B. *Chem. Phys. Lett.* **1999**, *313*, 795.
(21) Taylor, T. R.; Asmis, K. R.; Xu, C.; Neumark, D. M. *Chem. Phys. Lett.* **1998**, *297*, 133.
(22) Li, R. R.; Dapkus, P. D.; Thompson, M. E.; Jeong, W. G.; Harrison, C.; Chaikin, P. M.; Register, R. A.; Adamson, D. H. *Appl. Phys. Lett.* **2000**, *76*, 1689.
(23) Andreoni, W. *Phys. Rev. B* **1992**, *45*, 4203.
(24) Paulus, B.; Fulde, P.; Stoll, H. *Phys. Rev. B* **1996**, *54*, 2556.
(25) Tozzini, V.; Buda, F.; Fasolino, A. *Phys. Rev. Lett.* **2000**, *85*, 4554.
(26) Tozzini, V.; Buda, F.; Fasolino, A. *J. Phys. Chem. B* **2001**, *105*, 12477.
(27) Pattanayak, J.; Kar, T.; Scheiner, S. *J. Phys. Chem. A* **2002**, *106*, 2970.
(28) Blase, X.; De Vita, A.; Charlier, J.-C.; Car, R. *Phys. Rev. Lett.* **1998,** *80*, 1666.
(29) Jensen, F.; Toftlund, H. *Chem. Phys. Lett.* **1993**, *201*, 89.
(30) Seifert, G.; Fowler, P. W.; Mitchell, D.; Porezag, D.; Frauenheim, Th. *Chem. Phys. Lett.* **1997**, *268*, 252.
(31) Alexandre, S. S.; Mazzoni, M. S. C.; Chacham, H. *Appl. Phys. Lett.* **1999**, *75*, 61.
(32) Matxain, J. M.; Fowler, J. E.; Ugalde, J. M. *Phys. Rev. A* **2000**, *61*, 512. Matxain, J. M.; Fowler, J. E.; Ugalde, J. M. *Phys. Rev. A* **2000**, *62*, 553. Matxain, J. M.; Mercero, J. M.; Fowler, J. E.; Ugalde, J. M. *Phys. Rev. A* **2001**, *64*, 053201.
(33) Kent, P. R. C.; Towler, M. D.; Needs, R. J.; Rajagopal, G. *Phys. Rev. B* **2000**, *62*, 15394.
(34) Ceperley, D. M.; Alder, B. J. *Phys. Rev. Lett.* **1980**, *45*, 566.
(35) Foulkes, W. M. C.; Mitas, L.; Needs, R. J.; Rajagopal, G. *Rev. Mod. Phys.* **2001**, *73*, 33.
(36) Grossman, J. C.; Mitá×f0, L.; Raghavachari, K. *Phys. Rev. Lett.* **1995**, *75*, 3870. Erratum: *Phys. Rev. Lett.* **1995**, *76*, 1006.
(37) Filippi, C.; Umrigar, C. J. *J. Chem. Phys.* **1996**, *105*, 213.
(38) Porter, A. R.; Al-Mushadani, O. K.; Towler, M. D.; Needs, R. J. *J. Chem. Phys.* **2001**, *114*, 7795.
(39) Porter, A. R.; Towler, M. D.; Needs, R. J. *Phys. Rev. B* **2001**, *64*, 035320.
(40) Hood, R. Q.; Chou, M.-Y.; Williamson, A. J.; Rajagopal, G.; Needs, R. J.; Foulkes, W. M. C. *Phys. Rev. Lett.* **1997**, *78*, 3350.
(41) Kent, P. R. C.; Hood, R. Q.; Williamson, A. J.; Needs, R. J.; Foulkes, W. M. C.; Rajagopal, G. *Phys. Rev. B* **1999**, *59*, 1917.
(42) Leung, W.-K.; Needs, R. J.; Rajagopal, G.; Itoh, S.; Ihara, S. *Phys. Rev. Lett.* **1999**, *83*, 2351.
(43) Becke, A. D. *J. Chem. Phys.* **1993**, *98*, 5648.
(44) Hohemberg, P.; Kohn, W. *Phys. Rev.* **1964**, *136*, 3864.
(45) Lee, C.; Yang W.; Parr, R. G. *Phys. Rev. B* **1988**, *37*, 785.
(46) Becke, A. D. *Phys. Rev. A* **1988**, *38*, 3098.
(47) Ovcharenko, I.; Aspuru-Guzik, A.; Lester, W. A., Jr. *J. Chem. Phys.* **2001**, *114*, 7790.
(48) McLean A. D.; Chandler, G. S. *J. Chem. Phys.* **1980**, *72*, 5639.
(49) Krishnan, R.; Binkley, J. S.; Seeger, R.; Pople, J. A. *J. Chem. Phys.* **1980**, *72*, 650.
(50) Schleyer, P. v. R.; Maerker, C.; Dransfeld, A.; Jiao, H.; Hommes, N. J. v. E. *J. Am. Chem. Soc.* **1996**, *118*, 6317.
(51) Schleyer, P. v. R.; Jiao, H.; Hommes, N. J. v. E.; Malking, V. G.; Malkina, O. L. *J. Am. Chem. Soc.* **1997**, *119*, 12669.
(52) Anderson, J. B. *J. Chem. Phys.* **1976**, *65*, 4121.
(53) Moskowitz, J. W.; Schmidt, K. E.; Lee, M. A.; Kalos, M. H. *J. Chem. Phys.* **1982**, *77*, 349.
(54) Reynolds, P. J.; Ceperley, D. M.; Alder, B. J.; Lester, W. A., Jr. *J. Chem. Phys.* **1982**, *77*, 5593.
(55) Frisch, M. J.; Trucks, G. W.; Schlegel, H. B.; Scuseria, G. E.; Robb, M. A.; Cheeseman, J. R.; Zakrzewski, V. G.; Montgomery, J. A., Jr.; Stratmann, R. E.; Burant, J. C.; Dapprich, S.; Millam, J. M.; Daniels, A. D.; Kudin, K. N.; Strain, M. C.; Farkas, O.; Tomasi, J.; Barone, V.; Cossi, M.; Cammi, R.; Mennucci, B.; Pomelli, C.; Adamo, C.; Clifford, S.; Ochterski, J.; Petersson, G. A.; Ayala, P. Y.; Cui, Q.; Morokuma, K.; Malick, D. K.; Rabuck, A. D.; Raghavachari, K.; Foresman, J. B.; Cioslowski, J.; Ortiz, J. V.; Stefanov, B. B.; Liu, G.; Liashenko, A.; Piskorz, P.; Komaromi, I.; Gomperts, R.; Martin, R. L.; Fox, D. J.; Keith, T.; Al-Laham, M. A.; Peng, C. Y.; Nanayakkara, A.; Gonzalez, C.; Challacombe, M.; Gill, P. M. W.; Johnson, B. G.; Chen, W.; Wong, M. W.; Andres, J. L.; Head-Gordon, M.; Replogle, E. S.; Pople, J. A. *Gaussian 98*, revision A.7; Gaussian, Inc.: Pittsburgh, PA, 1998.
(56) Williamson, A. J.; Kenny, S. D.; Rajagopal, G.; James, A. J.; Needs, R. J.; Fraser, L. M.; Foulkes, W. M. C.; Maccullum, P. *Phys. Rev. B* **1996**, *53*, 9640.
(57) Umrigar, C. J.; Wilson, K. G.; Wilkins, J. W. *Phys. Rev. Lett.* **1988**, *60*, 1719.
(58) Kent, P. R. C.; Needs R. J.; Rajagopal, G. *Phys. Rev. B* **1999**, *59*, 12344.
(59) Needs, R. J.; Rajagopal, G.; Towler, M. D.; Kent, P. R. C.; Williamson, A. J. *CASINO*, version 1.0 User's Manual, University of Cambridge: Cambridge, U.K., 2000.
(60) Ceperley, D. M. *J. Stat. Phys.* **1986**, *43*, 815.
(61) Hammond, B. L.; Lester, W. A.; Reynolds, P. J. *Monte Carlo Methods in Ab Initio Quantum Chemistry*; World Scientific: Singapore, 1994.
(62) Lee, Y.; Kent, P. R. C.; Towler, M. D.; Needs, R. J.; Rajagopal, G. *Phys. Rev. B* **2000**, *62*, 13347.
(63) Greeff, C. W.; Lester, W. A., Jr. *J. Chem. Phys.* **1998**, *109*, 1607.
(64) Hurley M. M.; Christiansen, P. A. *J. Chem. Phys.* **1987**, *86*, 1069.
(65) Hammond, B. L.; Reynolds, P. J.; Lester, W. A., Jr. *J. Chem. Phys.* **1987**, *87*, 1130.
(66) Mitas, L.; Shirley, E. L.; Ceperley, D. M. *J. Chem. Phys.* **1991**, *95*, 3467.